Available free online at www.medjchem.com

Mediterranean Journal of Chemistry

Mediterranean Journal of Chemistry **2019**, 9(2), 155-163

Removal of methyl orange from aqueous solution using synthetic clay type MgAl-LDH: Characterization, Isotherm and thermodynamic studies

Ahmed Zaghloul, Abdeljalil Ait Ichou, Ridouan Benhiti, M'hamed Abali, Amina Soudani, Mohamed Chiban, Mohamed Zerbet and Fouad Sinan*

Laboratory LACAPE, Faculty of Science, University Ibn Zohr, BP. 8106, Hay Dakhla, Agadir, Morocco.

Abstract: The MgAl-LDH adsorbent (2:1) was developed by the urea method and used as an adsorbent for the removal of methyl orange from aqueous solution. The synthesized adsorbent was characterized by a different analytical technique: scanning electron microscope SEM, X-ray diffraction (XRD) and infrared spectroscopy (FT-IR). The effect of adsorption parameters such as solution pH, initial concentration of dye, and the temperature was studied using a static system. X-ray diffraction analysis of the samples confirms the crystal structure of the MgAl-LDH material. The MgAl-LDH adsorbent was efficient in removing MO from aqueous solution, and maximum removal of 98.5 % was observed in the pH range from 2 to 10. The maximum adsorption capacity of MgAl-LDH (2:1) was calculated from the Langmuir isotherm; the maximum quantity is 1250 mg. g^{-1}. The determination of the thermodynamic parameters indicates that the reaction between methyl orange and MgAl-LDH (2:1) is spontaneous and exothermic ($\Delta H°<0$ and $\Delta G°<0$).It can be concluded that LDH adsorbent can be used effectively for the removal of anionic dyes from industrial wastewater.

Keywords: Layered double hydroxides; Adsorption; Methyl orange; Wastewater treatment.

1. Introduction

Because of their accumulation (in both effluents and environment), the use of chemicals leads to severe environmental problems directly or indirectly (chronic toxicity) arising from these compounds or their degradation products. More than $7x10^5$ tons and about 10000 different types of dyes and pigments are produced every year around the world [1]. It is estimated that 10 to 15% of the dye is lost in the effluent [2].

Methyl orange (MO), which is widely used in dyeing industries, is known to be highly toxic, carcinogenic and mutagenic [3, 4]. Therefore, it is imperative to get rid of this dye from a waste stream before it is discharged into aqueous bodies. Various effluent treatment techniques such as adsorption [5], membrane filtration [6], chemical oxidation [7], ozonation [8], biological treatment [9], ion exchange [10], coagulation and flocculation [11] have been widely used to remove dyes and especially methyl orange from an aqueous medium. From all the processing techniques, adsorption is widely adopted because of its high removal efficiency, low process cost and easy to use. Various materials have been studied for adsorption reduction of dyes in wastewater. These materials include plants, activated carbon [12], chitosan [13], fly ash [14], rice husks [15], zeolites [16], ferrite nanoparticles [17]. In the current state, researchers' attention is directed towards the exploration of new adsorbents with high adsorption capacities for different pollutants. Lamellar double hydroxides (LDH), also called hydrotalcite clays or anionic clays, have been attracted attention in recent years because of its application in various fields, including the water treatment sector [18]. LDH has been considered as excellent adsorbents for wastewater treatment because of their large surface area, their layered structure and their interlayer ion exchange. It is efficient, inexpensive, simple, easy to perform and insensitive to toxic substances [18]. Previous works on dye adsorption [19,20] have proven their usefulness as adsorbents for some pollutants. Among the different types of LDH species, a compound consisting of a dual compound of MgAl-LDH hydroxides with carbonate as interlayer anions is commonly used for various applications [21, 22]. In this study, we synthesized a clay using the urea method; then, we characterized our adsorbent using various techniques, such as X-ray diffraction (XRD), Scanning Electron Microscopy (SEM), X-ray emission spectroscopy (EDX) and infrared spectroscopy (FT-IR), Batch adsorption experiments were performed to study the

*Corresponding author : Fouad Sinan
Email address: f.sinan@uiz.ac.ma
DOI: http://dx.doi.org/10.13171/mjc92190925728fs

Received August 20, 2019
Accepted August 27, 2019
Published September 25, 2019

effect of pH, initial MO concentration and temperature on the removal of MO from water. The adsorption equilibrium and thermodynamic parameters of MO on MgAl-LDH (2:1) were also discussed.

2. Materials and methods

2.1. Preparation of adsorbate

The Methyl orange used in this study was purchased from Panreac (Barcelona, Spain). A Stock solution of 1g. L^{-1} of methyl orange dye was prepared with double distilled water. The working solutions were obtained by diluting the stock solution. The molecular structure and some physicochemical characteristics of used dye are shown in Table 1.

Table1. Characteristics of Methyl orange.

Molecular structure	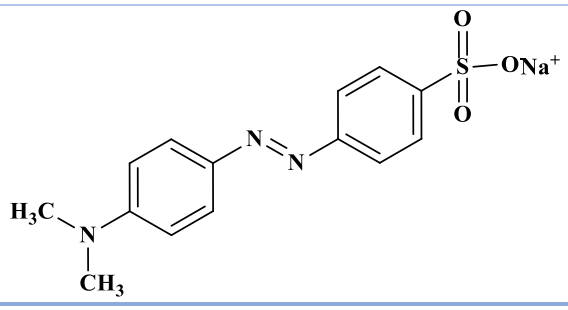
Chemical formula	$C_{14}H_{14}N_3NaO_3S$
λ max (nm)	464
Type of dye	Anionic
Molar mass (g. mol^{-1})	327.33

2.2. Preparation of MgAl-LDH

Urea is a fragile Brønsted base (pK_b =13.8), highly soluble in water, and its hydrolyzing rate may be controlled by the temperature, its decomposition giving rise to ammonium carbonate:

$$NH_2 - (C = O) - NH_2 + 2H_2O \rightarrow 2NH_4^+ + CO_3^{2-}$$

According to Shaw and Bordeaux [23] hydrolysis of urea proceeds in two steps, the formation of ammonium cyanate (NH_4CNO) as the rate-determining step, and the fast hydrolysis of the cyanate to ammonium carbonate.

The same conditions were described by Costantino et al. [24] were used to prepare MgAl-LDH: NH_2CONH_2 (AppliChem > 99%) is dissolved in an aqueous solution of $AlCl_3.6H_2O$ (AppliChem > 95%) and $MgCl_2.6H_2O$ (LobaChemie > 98%). Solid urea was added to 0.5 $mol.dm^{-3}$ metal solutions, having a molar ratio (Mg^{2+}/Al^{3+}) equal to 2, to reach urea/metal ions molar ratio of 3.3. The clear solution was refluxed and at 100°C to start the hydrolysis reaction. The pH was measured all along with the reaction with an industrial pH electrode for high temperature. The reaction was stopped after 36 hours, and the solids were separated from the solution and washed with distilled water.

2.3. Characterization of MgAl-LDH (2:1)

The crystalline structure of the obtained product was characterized by X-ray diffraction (D221-18-X-6 XRD-ray instrument, 2θ =11.50 ° to 65.94°) with CuK_α radiation (1.54 Å). The morphology observations were carried out on field emission scanning electron microscope (SEM, UATRS CNRST). FT-IR study was carried out using FTIR 8400S Shimadzu-FTIR spectra were recorded, in the range of 400–4000 cm^{-1} with KBr pellets technique.

2.4. Adsorption study of methyl orange

Adsorption experiments were evaluated in batch equilibrium mode. All experiments were conducted by mixing 40 mL of aqueous dye solutions with 20 mg of the adsorbent. The appropriate pH (2-12) of the mixture was adjusted using solutions of HCl (0.1N) and NaOH (0.1N). The adsorption isotherms were determined at 293.15 K with initial concentrations of MO (50–800 $mg.L^{-1}$). The temperature effect was achieved at (T=25, 30, 35°C) After stirring, the mixture was centrifuged at 3000 rpm for 15 minutes to separate the spent adsorbent from the residual dye. The equilibrium concentration of dye solution was measured using UV–vis spectrometer (UV-2005) at the max value of 464 nm for MO. The amount of dye adsorbed at equilibrium q_e (mg. g^{-1}) is given by the following equation:

$$q_e = \frac{(C_0 - C_e)}{m} \times V \quad (1)$$

With q_e is the equilibrium adsorption capacity ($mg.g^{-1}$), C_0 and Ce are the initial and equilibrium concentration ($mg.L^{-1}$) of MO in solution, m is the adsorbent mass (mg), V is the Volume of the solution (ml).

3. Results and Discussion

3.1. Characterization of Mg Al-LDH

Figure 1 shows the XRD diffractogram of MgAl-LDH. It indicates a high degree of crystallinity; these peaks were located at approximately 11.50°; 23.12°; 34. 89°; 39.36°. 46.58°;52.80°;56.06°; 60.75°; 62.03°.65.94° and can be assigned to plans (003);

(006); (012); (015); (018); (1010); (0111); (110); (113); (116). Various researchers have reported similar results [17, 25]. All diffraction peaks are indexed under a hexagonal structure and crystallized in a Rhombohedral crystal system with a spatial group R-3m, the number of pattern Z=1 and a density d =2.09. The interlayer d-spacing d_{003} and d_{006} of Mg-Al LDH were found to be 7.69 Å and 3.84 Å. The d_{003} was twice as much as d_{006}, suggesting a favorable layer structure [26].

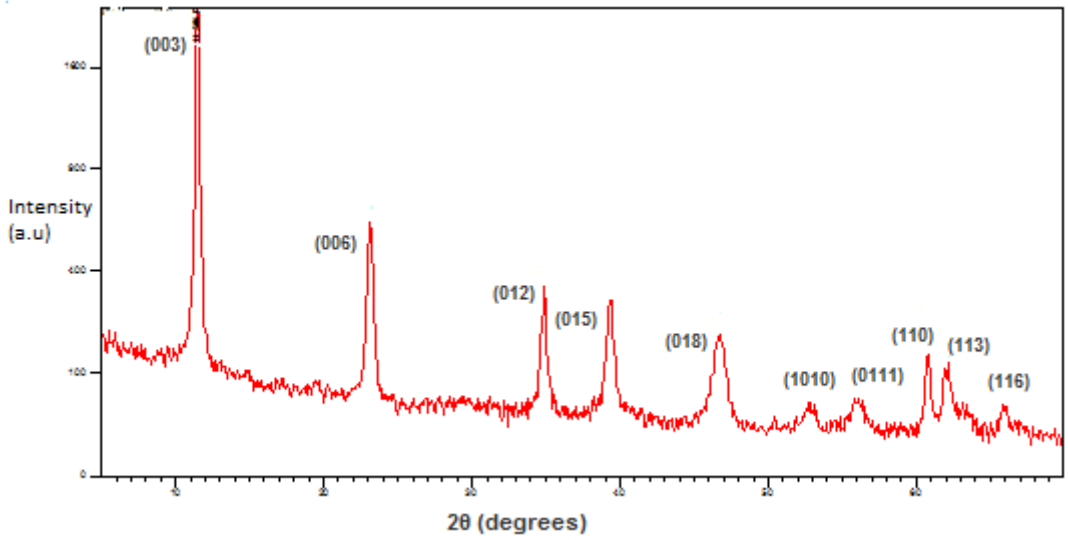

Figure 1. X-ray diffraction of MgAl-LDH

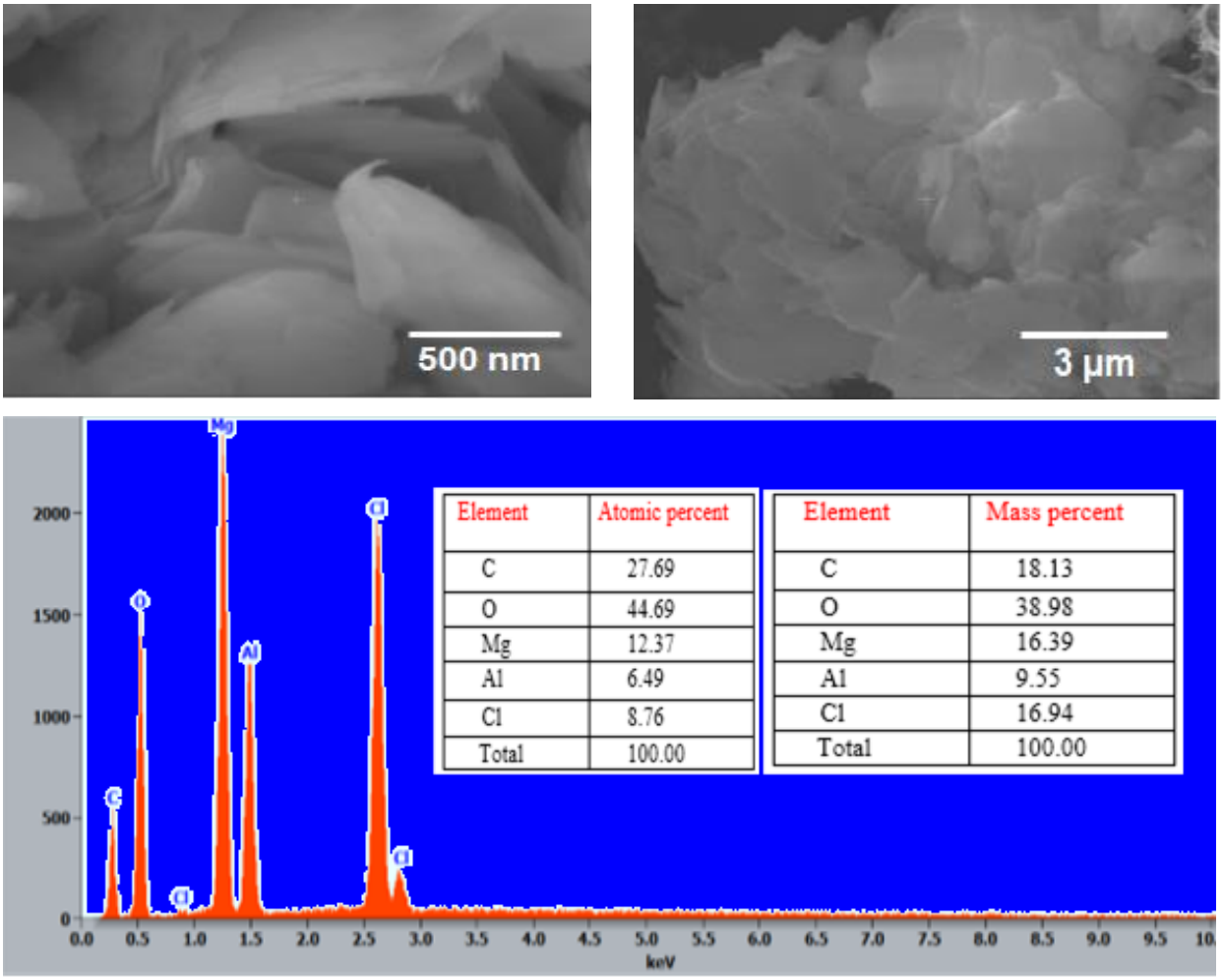

Element	Atomic percent
C	27.69
O	44.69
Mg	12.37
Al	6.49
Cl	8.76
Total	100.00

Element	Mass percent
C	18.13
O	38.98
Mg	16.39
Al	9.55
Cl	16.94
Total	100.00

Figure 2. SEM-EDS analysis of MgAl-LDH

Figure 2 presents the SEM-EDX; the two images present a morphology in the form of porous sheets. The surface of MgAl-LDH forms a compact hexagonal stack; similar studies are reported by [25,1]. The spectre (EDX) indicates the presence of magnesium, aluminium, chloride, the molar ratio of Mg /Al was 1.90 which is in a good agreement with the molar ratio (Mg^{2+}/Al^{3+}=2) used during the preparation of Mg Al-HDL (2:1).

Figure 3 displays the infrared spectra of the samples measured between 4000 and 400 cm^{-1}. The peak at 3453 cm^{-1}, related to the O-H stretching vibration v(O-H) of the metal hydroxide layer and interlayer water molecules [27]. The band at 2368 cm^{-1} is typically assigned to CO_2 from air [28]. The peak at 1615 cm^{-1} to the OH stretching band of H_2O [29]. The band observed at 1358 cm^{-1} is attributed to the stretching vibration of CO_3^{2-} [30]. The bands in the range of 542–779 cm^{-1} are attributed to M-oxygen-M stretching (M= Mg and Al) [31].

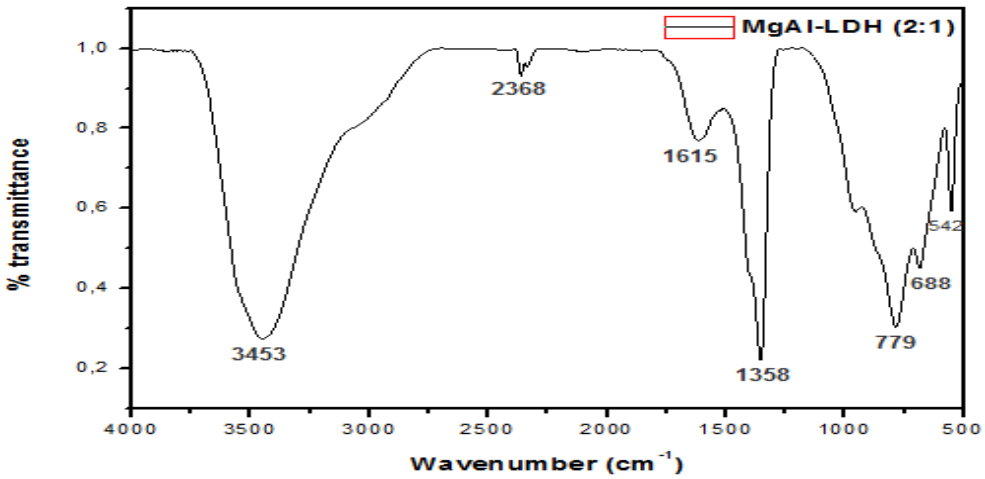

Figure 3. FTIR spectra of Mg-Al-LDH

3.2. Adsorption of methyl orange

3.2.1. Effect of initial pH on dye adsorption

The pH of the solution is one of the most important parameters in the adsorption process. Figure 4 shows the effect of the initial pH on the adsorption of MO over pH range (2 to 12). In the range of pH from 2 to pH=10, adsorption remains constant with an adsorption amount of 197 mg. g^{-1}, due to the strong electrostatic interactions between the solute (MO) and the positively charged H^+ surface of the adsorbent. For a pH value of 10, there is a decrease for adsorption explained by the competition between excess OH^- in a basic solution for adsorption sites with MO anions. A similar study of the elimination of MO by another adsorbent has been reported by other researchers [1, 32].

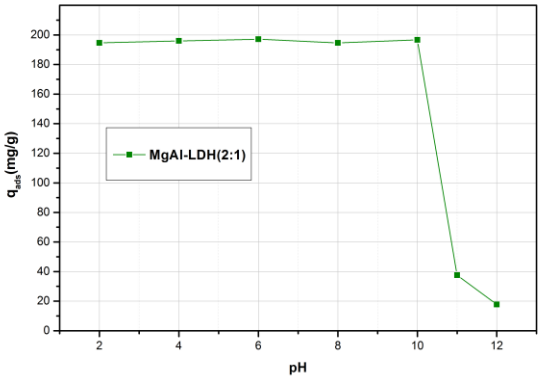

Figure 4. Effect of pH on adsorption of methyl orange (Ci=100mg/L, m=20mg, V=40ml, t=3h, T=25°C)

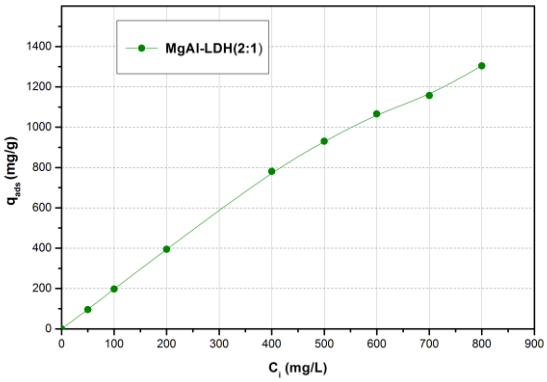

Figure 5. Effect of initial concentration of Methyl orange (m = 20 mg, V=40ml, t=3h, T=25°C)

3.2.2. Effect of initial MO concentrations

The effect of initial MO concentration on its removal by MgAl-LDH was studied at different concentrations ranging from 50 mg. L^{-1} to 800 mg. L^{-1} (Figure 5).

Analysis of this curve shows that the adsorbed amount of MgAl-LDH (2:1) increases with increasing initial concentration without reaching saturation.

3.2.3. Adsorption isotherm

To understand the mechanisms involved in the adsorption of MO on our material, we have sought to model the isotherms of adsorption (Figure 6) by applying the two most commonly used models: Langmuir and Freundlich. The Langmuir model (Figure 7A) is based on the assumption that the surface is uniform with no interactions between adsorbed molecules; and that, it has defined adsorption sites [33]. This model considers that adsorption takes place through the formation of an adsorbate monolayer and leads to the following equation:

$$q_e = q_m \times \frac{K_L \times C_e}{1 + K_L \times C_e} \quad (2)$$

With q_m : Capacity maximum adsorbed ($mg.g^{-1}$), K_L: adsorbent characteristic equilibrium constant ($L.\ mg^{-1}$), dependent on temperature and experimental conditions, C_e: adsorbate concentration at equilibrium ($mg.L^{-1}$).

The linearization of equation (2) leads to:

$$\frac{1}{q_e} = \frac{1}{q_m K_L}\frac{1}{C_e} + \frac{1}{q_m} \quad (3)$$

By plotting $\frac{1}{q_e}$ as a function of $\frac{1}{C_e}$ this gives a line of slope $\frac{1}{q_m K_L}$ and ordinate at the origin $\frac{1}{q_m}$ .The Freundlich isotherm is an empirical equation that assumes that the adsorption surface becomes heterogeneous during the adsorption process. The Freundlich isotherm (Figure 7 B) is expressed by the following equation [34]:

$$q_e = K_F C_e^{1/n} \quad (4)$$

Where k_F is a constant related to the binding energy, it can be defined as the adsorption or distribution coefficient and represents the amount of dye adsorbed on the adsorbent for the concentration unit at equilibrium. $\frac{1}{n}$ Indicates the dye adsorption intensity on the adsorbent or surface heterogeneity, which becomes more heterogeneous as the $\frac{1}{n}$ value approaches zero. A value of $\frac{1}{n}$ is below 1 indicates a normal Langmuir isotherm, while $\frac{1}{n}$ above 1 indicates a cooperative adsorption [35]. This equation can also be expressed as:

$$\mathrm{Ln} q_e = \frac{1}{n}\ \mathrm{Ln} C_e + \mathrm{Ln}\ K_F \quad (5)$$

The values of the constants of the adsorption isotherms with correlation coefficients are summarized in Table 2. The value obtained from R^2 of MgAl-LDH (2:1) for the Langmuir isotherm was 0.99 at 298 K, which is higher than that of the Freundlich isotherms. This indicated that the Langmuir isotherm fully describes the nature and sorption mechanism of MO on the composite studied. The maximum adsorption capacity of MgAl-LDH (2:1) calculated from the Langmuir isotherm was 1250 mg. g^{-1}. The result obtained from $\frac{1}{n}$ at 298 K was 0.34, indicating that the adsorption system o MO-MgAl- LDH (2:1) was favourable (i.e. (1< n <10).

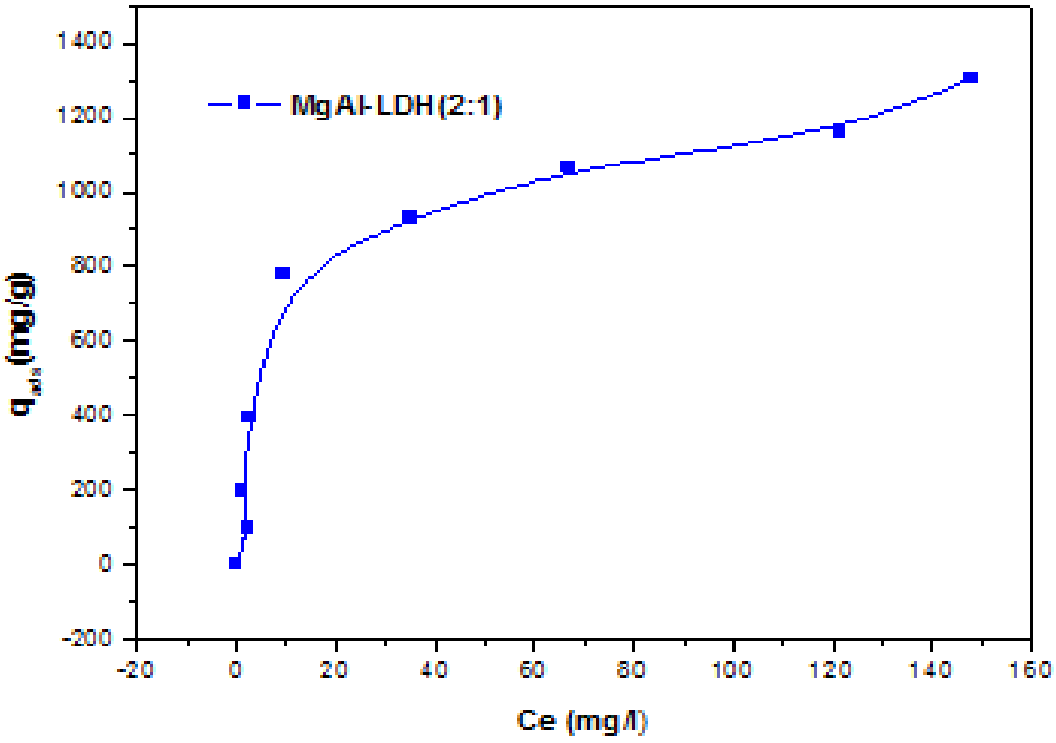

Fig 6. Isotherm of the adsorption of MO by MgAl- LDH (2:1) (m=20mg, V=40ml, t=3h, T= 25°C).

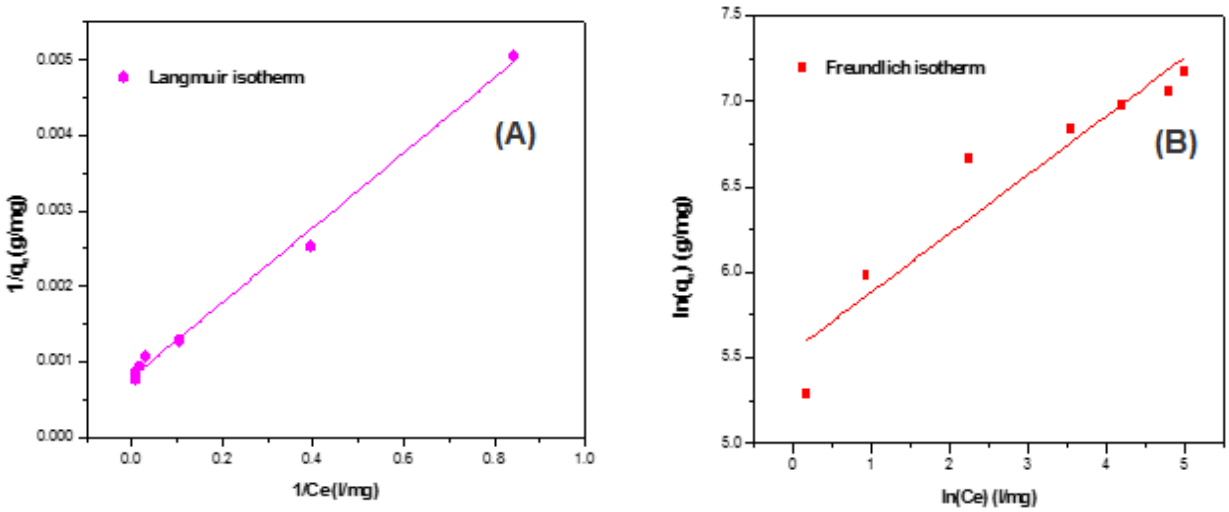

Figure 7. Linear plots of isotherm models of MgAl-LDH (2:1), Langmuir (A), Freundlich (B)

Table 2. Constants of Langmuir and Freundlich isotherm models for MO adsorbed by the MgAl- LDH

Langmuir			Freundlich		
q_m (mg.g^{-1})	K_L (L.mg^{-1})	R^2	K_F (mg.g^{-1})	1/n	R^2
1250	0.16	0.99	254.47	0.34	0.90

3.2.4. Effect of temperature and thermodynamic study

Adsorption is a phenomenon that can be endothermic or exothermic depending on the adsorbent material and the nature of the adsorbed molecules [36]. As shown in Figure 7, the adsorbed quantity of MO in both concentrations decreased slightly as temperature increases. Adsorption of MO onto MgAl-LDH(2:1) is an exothermic process; the adsorption capacity decreased with an increase in solution temperature.

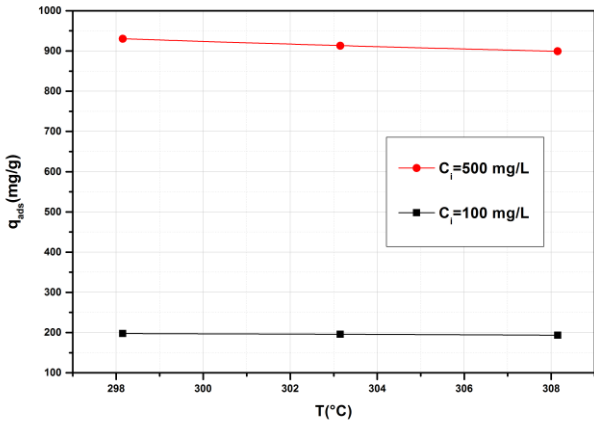

Figure 7. Effect of temperature on MO by MgAl-LDH (2:1), (m = 20 mg, V=40ml, t=3h)

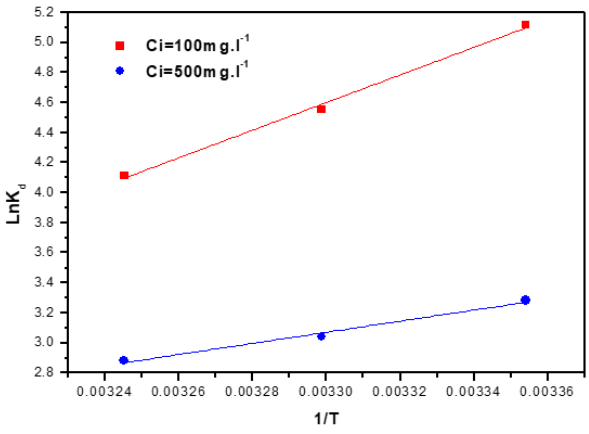

Figure 8. Linear plots of ln K_d vs $\frac{1}{T}$

Thermodynamic parameters such as standard Gibbs free energy (ΔG°) (kJ.mol^{-1}), standard entropy (ΔS°) (J.mol^{-1}.K^{-1})and standard enthalpy (ΔH°) (Kj.mol^{-1}) were determined using the following equations [1]:

$$K_d = \frac{q_e}{C_e} \quad (6)$$

$$\Delta G° = -RT \, Ln \, K_d \quad (7)$$

$$Ln \, K_d = \frac{\Delta S°}{R} - \frac{\Delta H°}{RT} \quad (8)$$

Where K_d (L.g^{-1}) is the thermodynamic equilibrium constant, T (K) is the temperature and R (8.314 J.mol^{-1}K^{-1}) is the universal gas constant, carrying ln K_d according to $\frac{1}{T}$ for both concentrations.

The linear curves of LnK_d concerning $\frac{1}{T}$ for the adsorption of MO on the MgAl-LDH composite (2:1) are shown in Figure 8, and the thermodynamic parameters are shown in Table 3. The negative values of ΔG° in Table 3 at all temperatures show that the adsorption of MO. on MgAl-LDH (2:1) was thermodynamically possible and spontaneous [37], for both concentrations, and the negative values of ΔH° indicated that the adsorption process was exothermic. Besides, the negative values of ΔS° indicated a more critical order of reaction during the adsorption, which can be attributed to the adhesion of the adsorbate with the adsorbent resulting in a decrease in the degree of freedom of the system [38].

Table 3. Thermodynamic parameters for MO adsorption on MgAl-LDH adsorbent (2:1).

C_i (mg.L^{-1})	T (K)	K_D	ΔG° (KJ.mol^{-1})	ΔS° (J.mol^{-1}.K^{-1})	ΔH° (KJ.mol^{-1})
100	298.15	166.22	-12.67	-214.23	-76.50
	303.15	95.05	-11.28		
	308.15	61.08	-10.19		
500	298.15	26.67	-8.13	-75.92	-30.74
	303.15	20.93	-7.66		
	308.15	17.84	-7.38		

3.2.5. Comparison with other adsorbents

The adsorption capacities of various adsorbents towards the adsorption of methyl orange, as reported in the literature presented in Table 4. Based on a comparison window between this work and other data reported in the literature, we found that our adsorbent (MgAl-LDH (2:1)) is a better adsorbent for MO removal.

Table 4. Adsorption capacity (q_{max}, mg. g^{-1}) of MO reported in the literature.

adsorbent	$C_{initial}$ (mg.L^{-1})	q_{max} (mg.g^{-1})	Reference
NiFe-LDH (2:1)	20-200	358.42	1
NiFe- LDH (1:1)	20-200	387.59	1
ZnMgAl–CO_3 LDH	10-100	683.9	39
NiFe- LDH	-	205.76	40
Lapindo volcanic mud	30-300	333.3	41
Zn/Al-LDO	50-200	181.9	42
MgNiAl	10-500	375.4	35
Activated alumina	-	9.8	43
Cork powder	-	16.66	44
MgAl- LDH (2:1)	50-800	1250	This study

4. Conclusion

In this study, a new material MgAl-LDH (2:1) was developed using the urea method; Different physicochemical techniques were used for LDH characterization such as Scanning Electron Microscopy (SEM), X-ray diffraction and infrared spectroscopy (FT-IR). The adsorbent was used to evaluate their adsorption capacity towards methyl orange. The optimum pH for the removal of MO was obtained in the pH range from 2 to10, the obtained results indicate that the adsorption of MO on the MgAl-LDH adsorbent (2:1) was better described by the Langmuir model with a good correlation (R^2=0.99) and a maximum adsorption amount (q_{max} =1250 mg.g^{-1}) on one hand. On the other hand, the thermodynamic data showed that the adsorption of the MO on the surface of MgAl-LDH (2:1) is of exothermic and spontaneous nature (ΔH°<0 and ΔG°<0). These exciting results offer several perspectives, such as the recycling of the material used. The synthesized carrier will also be tested for trapping other organic solvents.

References

1- M. Zubair, N. Jarrah, Ihsanullah, A. Khalid, M. Manzar, T. Kazeem, M. A. Al-Harthi, Starch-NiFe-layered double hydroxide composites: Efficient removal of methyl orange from the aqueous phase, Journal of Molecular Liquids, **2018**, 249, 254–264.

2- V.K. Gupta, R. Jain, T.A. Saleh., A Nayak, S. Malathi, S. Agarwal, Equilibrium and thermodynamic studies on the removal and recovery of Safranine-T Dye from industrial effluents, Sep. Sci. Technol, **2011**, 46, 839–846.

3- F. Ling, L. Fang, Y. Lu, J. Gao, F. Wu, M. Zhou, B. Hu, A novel CoFe layered double hydroxides adsorbent: high adsorption amount for methyl orange dye and fast removal of Cr (VI), Microporous Mesoporous Mater, **2016**. 234, 230–238.

4- B.H.A.I. Tan, T.T.O.W. Teng, A.K.M.O. M, Removal of dyes and industrial dye wastes by magnesium chloride, Water Res, **2000**, 34, 597–601.

5- A. Abbas, B.A. Abussaud, N.A.H. Al-Baghli, Ihsanullah. M, Khraisheh. M.A Atieh, Benzene removal by iron oxide nanoparticles decorated carbon nanotubes, J. Nanomater, **2016.**

6- M. Liu, Q. Chen, K. Lu, W. Huang, Z. Lü, C. Zhou, S. Yu, C. Gao, High efficient removal of dyes from aqueous solution through nanofiltration using diethanolamine-modified polyamide thin-film composite membrane, Sep. Purif. Technol, **2017**, 173, 135–143.

7- A. Uygur, Reuse of decolourised wastewater of azo dyes containing dichlorotriazinyl reactive groups using an advanced oxidation method, Color. Technol, **2001**, 117, 111–113.

8- K. Turhan, Z. Turgut, Decolorization of direct dye in textile wastewater by ozonization in a semi-batch bubble column reactor, Desalination, **2009,**242, 256–263.

9- A. Stolz, Basic and applied aspects in the microbial degradation of azo dyes, Appl. Microbiol. Biotechnol, **2001**, 56, 69–80.

10- C.H. Liu, J.S. Wu, H.C. Chiu, S.Y. Suen, K.H. Chu, Removal of anionic reactive dyes from water using anion exchange membranes as adsorbers, Water Res, **2007**, 41, 1491–1500.

11- F. Harrelkas, A. Azizi, A. Yaacoubi, A. Benhammou, M.N. Pons, Treatment of textile dye effluents using coagulation-flocculation coupled with membrane processes or adsorption on powdered activated carbon, Desalination, **2009**, 235 ,330–339.

12- F. Rozada, L.F. Calv, A.I. García, J. Martín-Villacorta, M. Otero, dye adsorption by sewage sludge-based activated carbons in batch and fixed-bed systems, Bioresour. Technol, **2003**, 87, 221–230.

13- M.S. Chiou, P.Y. Ho, H.Y. Li, Adsorption of anionic dyes in acid solutions using chemically cross-linked chitosan beads, Dyes Pigments, **2004**, 60, 69–84.

14- P. Janos, H. Buchtova, M. Rznarova, Sorption of dyes from aqueous solutions onto fly ash, Water Res, **2003**, 37, 4938–4944.

15-Y. Gou, S. Yang, W. Fu, J. Qi, R. Li, Z. Wang, H. Xu, Adsorption of malachite green on micro- and mesoporous rice husk-based active carbon, Dyes Pigments, **2003** 56, 219–229.

16- O. Ozdemir, B. Armagan, M. Turan, M.S. Çelik, Comparison of the adsorption characteristics of azo-reactive dyes on mesoporous minerals, Dyes Pigments, **2004**, 62, 49–60.

17- X. Wu, W. Wang, F. Li, S. Khaimanov, N. Tsidaeva, PEG-assisted hydrothermal synthesis of $CoFe_2O_4$ nanoparticles with enhanced selective adsorption properties for different dyes, Appl. Surf. Sci, **2016**, 389, 1003–1011.

18- F.L. Theiss, S.J. Couperthwaite, G.A. Ayoko, R.L. Frost, A review of the removal of anions and oxyanions of the halogen elements from aqueous solution by layered double hydroxides, J. Colloid Interface Sci, **2014**, 417, 356–368.

19- M. Zhu, Y. Li, M. Xie., H. Xin, Sorption of an anionic dye by uncalcined and calcined layered double hydroxides: a case study, J. Hazard. Mater, **2005**, 120, 163–171.

20- R. Bastiani, I.V. Zonno, I.A.V. Santos, C.A. Henriques, J.F.L. Monteiro, Influence of thermal treatments on the basic and catalytic properties of MgAl-mixed oxides derived from hydrotalcite, Braz. J. Chem. Eng, **2004**, 21,193–202.

21- O. Aschenbrenner, P. Guire, S. Alsamaq, J. Wang, S. Supasitmongkol, B. Al-Duri, P. Styring, J. Wood, Adsorption of carbon dioxide on hydrotalcite-like compounds of different compositions, Chem. Eng. Res. Des, **2011**, 89, 1711-1721.

22-W.T. Reichle, Synthesis of anionic clay minerals (mixed metal hydroxides hydrotalcite), Solid State Ionics, **1986**, 22, 135–141.

23- W.H.R. Shaw and J.J. Bordeaux, the Decomposition of Urea in Aqueous Media, J. Am. Chem. Soc., **1955**, 77, 4729

24- U. Costantino, F. Marmottini, M. Nocchetti, R. Vivani New Synthetic Routes to Hydrotalcite-Like Compounds, European journal of inorganic chemistry **1998** 1439-1446.

25- R. Elmoubarki, F. Mahjoubi, A. Tonsadi, M. Abdennouri, M. Sadiq, S. Qourzal, A. Zouhri, N. Barka. Ni/Fe and Mg/Fe layered double hydroxides and their calcined derivatives: preparation, characterization and application on textile dyes removal, Journal of Materials Research and Technology, **2017**, 3, 271-283.

26- D.G. Evans, R.C.T. Slade, Structural aspects of layered double hydroxides, J. Struct. Bond, **2006**, 119, 1-87

27- S. Aisawa, H. Hirahara, H. Uchiyama, S. Takahashi, and E. Narita, Synthesis and thermal decomposition of Mn-Al layered double hydroxides, J. Solid State Chem., **2002**, 167, 152–159

28- M. Yoshida, P. Koilraj, X. Qiu1, T. Hirajima, K. Sasaki, Sorption of arsenate on MgAl and MgFe layered double hydroxides derived from calcined dolomite, Journal of Environmental Chemical Engineering, **2015**, 2213-3437.

29- H.T. Kang, K. Lv, S.L. Yuan, Synthesis, characterization, and SO2 removal capacity of MnMgAlFe mixed oxides derived from hydrotalcite-like compounds, Appl. Clay Sci., **2013**, 72, 184-190.

30- O.P. Ferreira, O.L. Alves, D.X. Gouveia, A.G. Souza Filho, J.A.C. de Paiva, J. Mendes Filho, Thermal decomposition and structural reconstruction effect on Mg–Fe based hydrotalcite compounds, J. Solid State Chem., **2004**, 177, 3058–3069.

31- J.T. Kloprogge, R.L. Frost, Infrared and Raman spectroscopic studies of layered double hydroxides (LDHs), in V. Rives (Ed.), Layered Double Hydroxides: Present and Future, Nova Sci. Pub. Inc., New York, **2001**, pp. 139–192.

32- R. Huang, Adsorption of methyl orange onto protonated cross-linked chitosan, Arab. J. Chem, **2017**, 10, 24-32.

33- I. Langmuir, The constitution and fundamental properties of solids and liquids, J. Am. Chem. Soc., **1916**, 38, 2221-2295.

34- H.M.F. Freundlich, Uber die adsorption in losungen, Z. Phys. Chem., **1906**, 57, 385-47029.

35- H. Zaghouane-Boudiaf, M. Boutahala, L. Arab. Removal of methyl orange from aqueous solution by uncalcined and calcined MgNiAl layered double hydroxides (LDHs), Chemical Engineering Journal, **2012**, 187,142–149.

36- A. Aarfane, A. Salhi, M.El Krati, S. Tahiri, M. Monkade, E.K. Lhadi, M. Bensitel, Kinetic and thermodynamic study of the adsorption of Red195 and Methylene blue dyes on fly ash and bottom ash in an aqueous medium. J. Mater. Environ. Sci., **2014**, 5 (6),1927-193.

37- N, Dalhat., S.A. Haladu, N. Jarrah, M. Zubair, M.H. Essa, S.A. Ali, Polyaspartate extraction of cadmium ions from contaminated soil: evaluation and optimization using central composite design, J. Hazard. Mater, **2018**, 342, 58-68.

38- R, Shan, L, Yan, K, Yang, S, Yu, Y, Hao, H, Yu, B, Du, Magnetic Fe_3O_4/MgAl-LDH composite for effective removal of three red dyes from aqueous solution, Chem. Eng. J. **2014**, 252, 38–46.

39-Y.M. Zheng, N. Li. W, De Zhang, Preparation of nanostructured microspheres of ZnMg-Al layered double hydroxides with high adsorption property, Colloids Surf. A Physicochem. Eng. Asp, **2012**, 415, 195–201

40-Y. Lu, B. Jiang, L. Fang, F. Ling, J. Gao, F. Wu, High-performance NiFe layered double hydroxide for methyl orange dye and Cr (VI) adsorption, Chemosphere, **2016**, 152, 415-422.

41- A. Aishah, S. Jalil, S. Triwahyono, N. Hazirah Adam, M. Diana Rahim, A. Arif, N. Aziz, H. Hanis, N. Hairom, M. Aini, Razali., Mahani, A.Z. Abidin, M. Khairul, A. Mohamadiah, Adsorption of methyl orange from aqueous solution onto calcined Lapindo volcanic mud, J. Hazard. Mater, **2010**, 181, 755–762.

42- Z. Ni, S. Xia, L.Wang, F.Xing, G.Pan, Treatment of methyl orange by calcined layered double hydroxides in aqueous solution: adsorption property and kinetic studies, J. Colloid Interface Sci., **2007**, 316, 284–291.

43- Y. Iida, T. Kozuka, T. Tuziuti, K. Yasui, Sonochemically enhanced adsorption and degradation of methyl orange with activated aluminas, Ultrasonics, **2004**, 42 635–639.

44- F. Krika, F. Benlahbib, Removal of methyl orange from aqueous solution via adsorption on cork as a natural and low-cost adsorbent: equilibrium, kinetic and thermodynamic study of the removal process, Desalin. Water Treat, **2015**, 53, 3711–3723.